Published in final edited form as:
Genesis. 2009 March ; 47(3): 142–154. doi:10.1002/dvg.20470.

A New Mouse Model for Temporal- and Tissue-Specific Control of Extracellular Superoxide Dismutase

Yani Zou[1], **Chih-Hsin Chen**[1], **John R. Fike**[2], and **Ting-Ting Huang**[1,3,*]

[1] Department of Neurology and Neurological Sciences, Stanford University, Stanford, California

[2] Departments of Neurological Surgery and Radiation Oncology, University of California, San Francisco, California

[3] Geriatric Research, Education, and Clinical Center (GRECC), VA Palo Alto Health Care System, Palo Alto, California

Summary

The extracellular isoform of superoxide dismutase (EC-SOD, *Sod3*) plays a protective role against various diseases and injuries mediated by oxidative stress. To investigate the pathophysiological roles of EC-SOD, we generated tetracycline-inducible *Sod3* transgenic mice and directed the tissue-specific expression of transgenes by crossing *Sod3* transgenic mice with tissue-specific transactivator transgenics. Double transgenic mice with liver-specific expression of *Sod3* showed increased EC-SOD levels predominantly in the plasma as the circulating form, whereas double transgenic mice with neuronal-specific expression expressed higher levels of EC-SOD in hippocampus and cortex with intact EC-SOD as the dominant form. EC-SOD protein levels also correlated well with increased SOD activities in double transgenic mice. In addition to enabling tissue-specific expression, the transgene expression can be quickly turned on and off by doxycycline supplementation in the mouse chow. This mouse model, thus, provides the flexibility for on–off control of transgene expression in multiple target tissues.

Keywords

EC-SOD; TRE promoter; CamKII-tTA; LAP-tTA; transgenic mouse model

INTRODUCTION

Extracellular superoxide dismutase (EC-SOD) is an antioxidant enzyme located in the extracellular matrix and on cell surfaces throughout the body. Because of its critical location, EC-SOD is considered as the essential antioxidant defense outside of the cell. For instance, EC-SOD is highly expressed in the vascular walls and is the predominant form of SOD in the human aorta, constituting 70% of the total SOD activity in this tissue (Oury *et al*., 1996). Recent studies have highlighted the pathophysiological roles of EC-SOD in cardiovascular disorders [reviewed in (Fattman *et al*., 2003; Fukai *et al*., 2002)], lung diseases (Bowler and Crapo, 2002; Bowler *et al*., 2002), and neurological conditions (Fattman *et al*., 2003). In a recent study, we found that EC-SOD deficiency is associated with reduced neurogenesis in the subgranular zone of hippocampal dentate gyrus (DG) both before and after a modest dose of X-irradiation (Rola *et al*., 2007). Based on these data, we

*Correspondence to: Ting-Ting Huang, Department of Neurology and Neurological Sciences, Stanford University, Stanford, CA and GRECC, VAPAHCS, CA. tthuang@stanford.edu.

contend that a better understanding of the pathophysiological roles of EC-SOD will enhance our knowledge of the pathogenesis of various disease and injury conditions that involve a major contribution of EC-SOD.

Transgenic (Tg) and knockout (KO) mice are powerful tools for use in examining the physiological functions of various proteins. Currently, two human EC-SOD Tg mouse lines are available. The first is controlled by a human β-actin promoter (Oury *et al*., 1992), resulting in constitutive and ubiquitous transgene expression. The second is controlled by a human surfactant protein-C promoter, resulting in transgene expression that is constitutive but restricted to alveolar type II and nonciliated bronchial epithelial cells (Folz *et al*., 1999). Although both Tg lines have made important contributions to our understanding of the role of EC-SOD in various pathological conditions (Fattman *et al*., 2003, 2006; Ghio *et al*., 2002; Hu *et al*., 2006; Kang *et al*., 2003; Rabbani *et al*., 2005; Suliman *et al*., 2001), an inducible transgenic system would provide greater flexibility in controlling the availability of EC-SOD in a temporal- and tissue-specific manner. In the current study, we utilized a tetracycline-inducible system and generated two independent transgenic lines. Temporal- and tissue-specific expressions were tightly controlled in these two transgenic lines by the combination of tissue-specific transactivators and doxycycline (Dox) supplementation. The EC-SOD produced from the transgenes is biologically active and appears to have a binding affinity to heparin that is similar to that of endogenous EC-SOD.

RESULTS

In Vitro Testing of EC-SOD Expression Constructs

A dicistronic expression construct (CMV-*Sod3*-GFP) with mouse EC-SOD (*Sod3*) cDNA fused with a sequence encoding hemagglutinin (HA) epitope (*Sod3*/HA) and the green fluorescence protein (GFP) gene under the control of a cytomegalovirus (CMV) promoter was generated using the pIRES-hrGFP-1a vector (Fig. 1a). To test the expression of *Sod3*/HA, CMV-*Sod3*-GFP was transfected into the mouse neuroblastoma cell line Neuro2A (ATCC, Manassas, VA). Strong expression of EC-SOD was first detected at 24 h after transfection and continued to 48 h (Fig. 1c). Moreover, EC-SOD, which was cleaved and released from the cell membrane, was detected in the culture medium 48 h after transfection (Fig. 1c), indicating that the EC-SOD transgene product underwent a natural cleavage process.

The fragment containing *Sod3*/HA-GFP was then inserted downstream of a tetracycline inducible promoter (TRE) using pTRE-Tight vector to generate TRE-*Sod3*-GFP construct (Fig. 1b). To test the inducible expression of TRE-*Sod3*-GFP in vitro, the construct was transfected into Tet-On 293 cells (Clontech, Palo Alto, CA). The expression of EC-SOD responded in a dose-dependent manner in transfected cells treated with Dox; no EC-SOD was detected in transfected cells exposed to no Dox treatment (Fig. 1d).

Heparin Binding Affinity of EC-SOD Produced by CMV-*Sod3*-GFP

The C-terminus of EC-SOD mediates the binding to both heparin/heparin sulfate and collagen in tissues and cells in culture. However, it is not clear if the addition of extra amino acids, such as the HA epitope used in this study, at the C-terminus will affect the binding affinity and consequently, the ratio between tissue-bound and circulating EC-SOD. To address this question, we used Heparin-Sepharose chromatography to assess the binding affinity of EC-SOD to heparin in a Neuro2A cell line stably transfected with CMV-*Sod3*-GFP (EC-SOD/HA). Protein extracts from mouse lungs were used as controls for the affinity binding of native EC-SOD. The majority of EC-SOD from lung homogenates eluted between 300 and 400 mM NaCl (see Fig. 2), whereas EC-SOD from Neuro2A cell lysates

eluted in a narrower range between 350 and 400 mM NaCl (see Fig. 2). This shows that EC-SOD/HA has a similar elution pattern as the native EC-SOD, suggesting that the HA epitope at the C-terminus of EC-SOD/HA does not affect the heparin binding affinity.

Control of TRE-*Sod3*-GFP by Transactivator Transgenic Mice

A total of 32 mice were obtained after DNA microinjection and two independent TRE-*Sod3*-GFP founder lines were identified (designated as #5 and #32, respectively) by PCR genotyping. Both lines demonstrated consistent transmission of the transgenes over six generations at the expected Mendelian ratio from both male and female breeders. No overt abnormalities were observed in animals from either transgenic line up to 3 months of age.

To test the tissue-specific control of TRE-*Sod3*-GFP expression, we crossed both transgenic lines with two transactivator (tTA) transgenics driven by liver-enriched activator protein promoter (LAP-tTA) (Kistner *et al*., 1996) and calcium-calmodulin-dependent kinase II promoter (CamKII-tTA) (Mayford *et al*., 1996), and one reverse transactivator, CamKII-rtTA (Mansuy *et al*., 1998), transgenic line available in our facility. Together, they provide opportunities to assess TRE-*Sod3*-GFP expression in the liver and forebrain neurons. The liver-specific transactivator Tg mouse LAP-tTA drives TRE-*Sod3*-GFP expression in the absence of Dox (Tet-Off system). We first determined the expression pattern of TRE-*Sod3*-GFP in a number of different organs in TRE-*Sod3*-GFP/LAP-tTA double Tg mice using western blot analysis. No difference in EC-SOD level was detected among nontransgenic (WT), TRE-*Sod3*-GFP single Tg (Tg/−), LAP-tTA single Tg (−/Tg), and TRE-*Sod3*-GFP/LAP-tTA double Tg (Tg/Tg) mice in brain, tongue, aorta, heart, spleen, pancreas, kidney, testis, uterus, muscle, and adipose tissue (data not shown). In liver, a slight increase in total EC-SOD was detected in Tg/Tg mice; however, no over expression was observed in Tg/− and −/Tg mice when compared with WT controls (Fig. 3a). When probed with HA antibody, strong signal was only detected in Tg/Tg mice and the signal was not detected in WT or either of the single Tg mice. This result indicated that there was no “leakage” in transgene expression in nontarget organs in Tg/Tg mice. There was also no leaky expression in single Tg mice, suggesting that single Tg mice can be used as suitable control animals. The two individual Tg lines #5 and #32 showed similar expression levels (Fig. 3a). We also examined the expression using anti-hr-GFP antibody; however, the signal was too weak to be detected. This could be due to the different expression ratio between genes up and down stream of the IRES sequence.

Given that a high percentage of hepatic EC-SOD is naturally cleaved by furin and released into circulation (Bowler *et al*., 2002), we wanted to determine if the EC-SOD transgene product underwent the same process and could be detected in plasma. The result showed that total EC-SOD levels were very high in plasma from Tg/Tg mice when compared with that from WT and single Tg mice (Fig. 3b). The circulating EC-SOD was also detected by anti-HA anti-body (Fig. 3b). In fact, the majority of EC-SOD in TRE-*Sod3*-GFP/LAP-tTA mice was processed and released into the circulation (Fig. 3b), leaving very little as the intact tissue bound form. This finding indicates that EC-SOD expression in TRE-*Sod3*-GFP/LAP-tTA double Tg mice can be determined by direct blood sampling.

To test the inducible expression of TRE-*Sod3*-GFP in forebrain neurons, we crossed TRE-*Sod3*-GFP Tg mice with two neuronal-specific transactivator Tg lines: CamKII-tTA (Tet-Off) and CamKII-rtTA (Tet-On). The level of EC-SOD expression in different brain areas was first determined in the Tet-Off system in TRE-*Sod3*-GFP/CamKII-tTA double Tg mice without Dox treatment. No increased expression of EC-SOD was observed either in the brain stem, cerebellum, or thalamus in Tg/Tg mice. On the other hand, the level of EC-SOD was significantly elevated in hippocampus and cortex in Tg/Tg mice when compared with single Tg controls (Fig. 4a). Both lines #5 and #32 showed similar expression patterns (Fig.

4a), and there was no difference in the expression level of EC-SOD between WT, Tg/−, and −/Tg mice (data not shown). These data implied that the expression of EC-SOD transgene in TRE-*Sod3*-GFP/CamKII-tTA was restricted to the forebrain region. We then determined the level of EC-SOD expression in the Tet-On system in TRE-*Sod3*-GFP/CamKII-rtTA double Tg mice fed with Dox-supplemented mouse chow to induce transgene expression. Double Tg and control mice (including WT and single Tg) were sacrificed after 2, 4, and 8 weeks on the Dox-supplemented diet to determine EC-SOD expression in different areas of brain. No change in EC-SOD expression was observed in any of the brain regions examined (data not shown), suggesting that the combination of TRE-*Sod3*-GFP and CamKII-rtTA was not an effective way for controlling EC-SOD expression in the brain.

To determine the tissue localization of EC-SOD produced by TRE-*Sod3*-GFP in the brain, we carried out immunofluorescence staining to detect and compare levels of EC-SOD in TRE-*Sod3*-GFP/CamKII-tTA double Tg and EC-SOD KO mice. Strong staining of EC-SOD was observed in the Cornu Ammonis area 1 (CA1), CA3, and DG in the hippocampal formation of TRE-*Sod3*-GFP/CamKII-tTA double Tg mice (Fig. 5, left panels). Further, the EC-SOD signals colocalized well with the neuronal marker neuronal nuclei (NeuN), indicating the neuronal origin of EC-SOD (Fig. 5, left panels). When compared with EC-SOD KO, although there was some nonspecific binding in KO mouse (Fig. 5, right panels), the EC-SOD labeling in Tg/Tg was much stronger, especially in CA1 and CA3 regions.

Increased SOD Activity is Detected in TRE-*Sod3*-GFP/tTA Double Transgenic Mice

To determine if the HA-tagged EC-SOD was biologically active, we measured SOD activity using the NBT method (Spitz and Oberley, 1989). In liver homogenates, SOD activity of TRE-*Sod3*-GFP/LAP-tTA double Tg mice was not higher than that of WT controls (data not shown). This could be due to the high level of CuZnSOD in the liver, which can mask the increase in EC-SOD activity in Tg/Tg mice. We also measured SOD activity in the plasma which should contain no CuZnSOD or MnSOD. The mean total SOD activity in controls (WT and single Tg) and Tg/Tg mice was 10.95 ± 4.01% IHB ($N = 7$) and 43.11 ± 4.87% IHB ($N = 6$), respectively. These results showed a 3.9-fold increase of SOD activity in Tg/Tg mice ($P < 0.001$, Fig. 3c), which correlated well with increased SOD protein level in plasma. Because of the limited quantity of plasma that could be collected from each mouse, cyanide inhibition assay was not carried out. Instead, western blot analyses were carried out to assess the extent of CuZnSOD and MnSOD contamination in the plasma, and no detectable signals were identified in any samples examined (data not shown). Therefore, the increase in plasma SOD activity in Tg/Tg mice could only be attributed directly to the increase in EC-SOD.

To determine the biological activity of EC-SOD in TRE-*Sod3*-GFP/CamKII-tTA double Tg mice, we isolated EC-SOD from cortex homogenates using a Concanavalin A (Con A) column (Marklund, 1984a, 1990). The eluted fractions from the column were determined to contain EC-SOD and were free of CuZnSOD and MnSOD contamination by western blot analysis (data not shown). The protein-containing fractions were pooled and used for SOD activity measurements after being concentrated through Microcon filter units. The mean SOD activity in control samples (WT and single Tg) was 0.08 ± 0.02 U/mg protein ($N = 3$) and in Tg/Tg was 0.51 ± 0.10 U/mg protein ($N = 3$). This showed a 6.4-fold increase of SOD activity in the cortex of Tg/Tg mice ($P = 0.01$, Fig. 4b), and correlated well with increased SOD protein level in the cortex. Because a precise measurement of EC-SOD requires passing tissue homogenates through affinity columns, large quantities of tissue are needed, making it difficult, if not impossible, to measure EC-SOD activities directly from mouse hippocampi which weigh about 10 mg each. However, because EC-SOD protein levels in the hippocampus are similar to that in cortex in TRE-*Sod3*-GFP/CamKII-tTA double Tg

mice, it is reasonable to expect a similar level of increase in EC-SOD activity in the hippocampal formation in Tg/Tg mice.

Dox-Mediated Suppression of TRE-*Sod3*-GFP Expression in TRE-*Sod3*-GFP/LAP-tTA and TRE-*Sod3*-GFP/CamKII-tTA Mice

To suppress TRE-*Sod3*-GFP expression in the Tet-Off system, control, TRE-*Sod3*-GFP/LAP-tTA and TRE-*Sod3*-GFP/CamKII-tTA mice were fed Dox-supplemented mouse chow (1,000 ppm) for specified intervals, and EC-SOD levels were determined in the plasma or brain (cortex and hippocampus). In TRE-*Sod3*-GFP/LAP-tTA mice, plasma EC-SOD levels were lowered after 3 days and completely reduced to that of the control level after 6 days of Dox treatment (see Fig. 6). In TRE-*Sod3*-GFP/CamKII-tTA mice, EC-SOD levels in both hippocampus and cortex were substantially lowered after 4 days and completely reduced to that of control level after 8 days of Dox treatment (Fig. 7a). To test the reversibility of Dox-mediated suppression of TRE-*Sod3*-GFP expression, TRE-*Sod3*-GFP/CamKII-tTA mice were fed Dox-supplemented mouse chow for 12 days to ensure a complete suppression. The mice were then switched back to regular mouse chow. Samples collected at 13 and 25 days after switching back to normal mouse chow showed a partial and complete recovery in EC-SOD expression in hippocampus and cortex, respectively (Fig. 7b).

DISCUSSION

In the present study, we created two independent lines of Tet-inducible EC-SOD Tg mice using a TRE-*Sod3*-GFP expression construct. The TRE-*Sod3*-GFP Tg mice showed tissue specific expression in liver and forebrain when driven by LAP-tTA and CamKII-tTA, respectively. In addition, the on–off control of transgene expression can be effectively regulated by Dox supplementation in mouse chow. EC-SOD encoded by HA-tagged *Sod3* is biologically active, and 3.9- and 6.4-fold increases in EC-SOD activity were observed in plasma and cortex, respectively, in Tg/Tg mice with liver- and neuronal-specific expression. The level of increase, insofar as the neuronal-specific expression is concerned, should be enough to be functionally significant because the level is comparable with that of an existing EC-SOD transgenic line (Oury *et al*., 1992) which has been shown to be more resistant to focal and global cerebral ischemia and cold induced brain edema (Oury *et al*., 1993; Sheng *et al*., 1999, 2000) and age-related decline in spatial memory (Hu *et al*., 2006).

Several considerations went into the design of TRE-*Sod3*-GFP expression construct. First, to avoid the commonly encountered leakiness in Tet-inducible Tg mice (Thomas *et al*., 2001; Zheng *et al*., 2000), we used a modified TRE promoter, p-Tight, which had been shown to have extremely low basal level expression and, at the same time, provided highly controlled inducible expression of target genes. The lack of leaky expression in both the in vitro (Fig. 2b) and in vivo systems confirms the effectiveness of the p-Tight promoter. Second, an HA-epitope was added to the C-terminus of EC-SOD. This allowed us to distinguish endogenously produced EC-SOD from the protein produced by the transgenes using an anti-HA antibody. Third, an IRES-GFP reporter gene was placed downstream of *Sod3*/HA and was controlled by the same TRE promoter. This provided a quick, visual confirmation of EC-SOD expression from the TRE promoter. GFP expression was high enough in transiently transfected Tet-On 293 cells for a direct observation under a fluorescent microscope (data not shown), but unfortunately was not high enough in tissue sections to allow a visual confirmation of TRE promoter activity.

To distinguish expression of the EC-SOD transgene from that of endogenous gene in various tissues, we tagged an HA-epitope to the C-terminus of transgenic EC-SOD. There was an initial concern about the location of the HA epitope due to the natural secretory process of EC-SOD in cells. As the signaling peptide for secretion of EC-SOD to the outer surface of

plasma membrane resides at the N-terminus, HA epitope at the N-terminus may not be present in the mature protein when the signaling peptide is cleaved. On the other hand, the last 15 amino acids at the C-terminus can be proteolytically cleaved by furin (Bowler *et al*., 2002) and released into circulation. Consequently, HA-epitope at the C-terminus may be removed from the circulating EC-SOD, resulting in an undetectable level in circulation by HA-antibody. The fact that we were able to detect the circulating EC-SOD by HA-antibody suggested that the circulating EC-SOD tetramers still contained the intact form, albeit at a much lower level than the cleaved form (Fig. 3b). The data also implied that we will be able to utilize HA-epitope to distinguish EC-SOD expression between transgenes and endogenous genes in all tissues.

The most important feature of TRE-*Sod3*-GFP Tg mice is the temporal- and tissue-specific control of transgene expression. We successfully used two established transactivator (Tet-Off) transgenic lines, LAP-tTA and CamKII-tTA, to drive the expression of TRE-*Sod3*-GFP in this study. Both transactivator transgenics have been shown to direct high level, tissue-specific expression of their target genes (Kistner *et al*., 1996; Mansuy et al., 1998; Mayford *et al*., 1996). The double Tg mice generated in this study quickly responded to Dox suppression in as much as it took only 3–4 days to see a significant suppression of TRE-*Sod3*-GFP expression in liver and forebrain (Figs. 6 and 7). Although we did not test the in vivo dose response to Dox, the in vitro experiments with Tet-On 293 cells showed a strong correlation between TRE-*Sod3*-GFP expression level and the dosage of Dox supplementation. Therefore, it is conceivable that similar dose responses can be achieved in the in vivo system. We also showed that Dox-mediated suppression of TRE-*Sod3*-GFP expression was reversible in TRE-*Sod3*-GFP/CamKII-tTA double Tg mice (Fig. 7b). By 13 days after the withdrawal of Dox from mouse chow, we observed almost complete recovery of TRE-*Sod3*-GFP expression in double Tg mice and the level remained stable. We have also tried to recover the expression of EC-SOD from TRE-*Sod3*-GFP/LAP-tTA double Tg mice. However, even at 2 months after the removal of Dox, EC-SOD expression was still suppressed to a low level. This may be due to the high level of Dox used in the initial suppression which was performed in immature mice. Dox can be easily incorporated into bones (van der Bijl and Pitigoi-Aron, 1995) and may be released to circulation later during bone restructuring.

Compared with the existing EC-SOD Tg mice, TRE-*Sod3*-GFP provides a greater flexibility in controlling expression in a temporal- and tissue-specific manner in multiple tissues and cell types without the need to generate individual tissue-specific Tg mice. Currently, different multiple tTA and rtTA driver lines are available for controlling TRE-mediated expression specifically in different tissues and cells, such as skeletal muscle (Grill *et al*., 2003), heart (Passman and Fishman, 1994), lung (Tichelaar *et al*., 2000), endothelial cells (Sarao and Dumont, 1998), smooth muscle cells (Li *et al*., 1996; West *et al*., 2004), and glia (Wang *et al*., 2004). Near ubiquitous expression is also possible by using a methylation-free CpG island (Katsantoni *et al*., 2007). TRE-*Sod3*-GFP can also be combined with EC-SOD KO mice, thereby, providing a greater range of EC-SOD levels (e.g., from 0 to several fold higher than endogenous levels) for examining the role of EC-SOD under different pathophysiological conditions.

A naturally occurring Arg213→Gly polymorphism in human EC-SOD exists in general populations and leads to a 10-fold increase in the serum level of EC-SOD (Sandstrom *et al*., 1994). Whereas the presence of the Gly allele has been associated with an increased risk for ischemic heart disease (IHD) in the Copenhagen City Heart Study (Juul *et al*., 2004), the presence of the Gly allele has also been shown to protect against the development of chronic obstructive pulmonary disease (COPD) in cigarette smokers (Juul *et al*., 2004, 2006). Therefore, TRE-*Sod3*-GFP/LAP-tTA mouse, with its high level of circulating EC-SOD, may

be useful as a model to decipher the role of bound vs. circulating EC-SOD in the development of IHD and COPD. Furthermore, high levels of EC-SOD in the brain have been shown to protect against age-mediated decline of learning and memory in aged EC-SOD Tg mice (Hu *et al*., 2006), and yet high levels of EC-SOD in young mice impair learning and memory (Thiels *et al*., 2000). These conflicting findings imply that age-specific physiological conditions may determine if antioxidant treatment can be beneficial or counterproductive. Therefore, the ability to increase EC-SOD only when and where needed, using the TRE-*Sod3*-GFP system, can enhance our ability to design and implement better intervention strategies or to identify important biochemical pathways involved in age-related changes in physiology.

METHODS

Generation of Transgenic Construct

The TRE-*Sod3*-GFP transgenic construct was generated by a three-step cloning process. A 756 bp full-length mouse *Sod3* cDNA was isolated by PCR from IMAGE clone 3983917 (Catalog number MMM1013-64823, Open Biosystems, Huntsville, AL). The PCR primers (up stream, 5′-CGC GAA TTC ATG TTG GCC TTC TTG TTC TA-3′; downstream, 5′-CGC TCG AGT TAG GCG TAG TCG GGC ACG TCG TAG GGG TAA GTG GTC TTG CAC TC -3′) were designed to provide an EcoR I site at the 5′ end and an Xho I site at the 3′ end. An HA epitope (HA-tag, YPYDVPDYA) was also engineered into the C-terminus of EC-SOD to provide an additional option for immunodetection of transgene expression. Sequences flanking the *Sod3* PCR cloning sites were sequenced to avoid clones with PCR artifacts. The *Sod3*/HA fragment was inserted into pIRES-hrGFP-1a expression vector (Stratagene, La Jolla, CA), between the CMV promoter and the GFP reporter. The *Sod3*/HA-IRES-GFP cassette (Fig. 1a) was then isolated as an EcoR I/Mlu I fragment and placed downstream from the TRE promoter in the pTRE-Tight expression vector (Fig. 1b) (Clontech, Mountain View, CA).

Generation of TRE-*Sod3*-GFP Transgenic Mice

For the generation of transgenic mice, the 3.4 kb DNA fragment containing TRE-*Sod3*-GFP (Fig. 1b) was isolated as a Sca I/Mlu I fragment by agarose gel electrophoresis and purified by QIAquick gel extraction kit (Qiagen, Valencia, CA). The DNA fragment was microinjected into B6CBAF1 embryos by the Transgenic Mouse Research Facility at Stanford University. Tail DNA was used for PCR genotyping of TRE-*Sod3*-GFP Tg mice, and the following primers were used: forward, 5′-GAA TTC ATG TTG GCC TTC TTG TTC TA-3′ and reverse, 5′-GTC CTT ATC ATC GTC GTC TT-3′. The PCR product was 846 bp in size. The *Sod2* (MnSOD) gene was used as the internal control with forward primer, 5′-GTC CCC CAC CAT TGA ACT T-3′ and reverse primer, 5′-GGG GCA TCT AGT GGA GAA GT-3′. The PCR product was 457 bp in size. The PCR reaction included 1× ThermoPol buffer (New England Biolabs, Ipswich, MA), 200 μM of each dNTP, 0.2 μM of each primer pair, and 0.5 U of Taq DNA Polymerase (New England Biolabs). The PCR mixture was heated for 5 min at 95°C for a hot start, followed by 35 cycles of 95°C for 30 s, 62°C for 1 min, and 72°C for 1 min, with a final extension step at 72°C for 7 min. PCR genotyping for tTA and rtTA Tg mice was carried out using the following primers: forward, 5′-GGT GTA GAG CAG CCT ACA TT-3′, and reverse, 5′-TTC TGT AGG CCG TGT ACC T-3′. The PCR product was 219 bp. The *Gfap* (glial fibrillary acidic protein) gene was used as an internal control with forward primer, 5′-GCG CGC TCG TGC ACA CTT ATC ACA C-3′ and reverse primer, 5′-CTG CCC CTG ACT TCC TGG AAG CAC-3′. The PCR product was 490 bp in size. The PCR condition was the same as that for TRE-*Sod3*-GFP. All animal handling procedures were approved by the IACUC committee at the VA Palo Alto Health Care System.

Western Blot Analysis for Quantification Of Transgene Expression

Sample preparation—Tissues were homogenized in four volumes (w:v = 1:4) of T-PER tissue protein extraction reagent (Pierce, Rockford, IL) containing Complete® protease inhibitor cocktail (Roche Applied Science, Indianapolis, IN) according to manufacturer's instruction. The samples were then centrifuged at 10,000 *g* at 4°C for 5 min and the supernatants stored in 20 μl aliquots at −80°C. Protein concentration of each sample was measured in triplicate using the BCA Protein Assay Reagent (Pierce).

Western blot analysis—Equal amounts of protein (cortex and hippocampus at 50 μg each, liver at 40 μg, plasma at 1 μl) from each sample were separated by NuPAGE 4–12% Bis-tris Gel (Invitrogen, Carlsbad, CA) followed by transferring to nitrocellulose membranes (Bio-Rad, Hercules, CA). A custom-made rabbit polyclonal antibody (Proteintech Group Inc., Chicago, IL) against a synthetic peptide (SNPGESSFDLADRLDPVEK), corresponding to amino acid 20–31 in the precursor protein of mouse EC-SOD, was used at 1 μg/ml. Anti-HA antibody was used at 1:10,000 (H 9658, Sigma, St. Louis, MO). Protein bands were visualized using DuoLuX Chemiluminescent/ Fluorescent Substrate Kit (Lumigen, Southfield, MI) after incubation with HRP-conjugated secondary antibody. All blots were reprobed with an antibody against β-actin (A3854, anti-β-actin-Peroxidase, 1:50,000; Sigma) and albumin (A90–134A, 1:10,000, Bethyl Laboratories, Inc., Montgomery, TX) as a loading control for tissue homogenates and plasma, respectively. Quantification of western blot results was done by normalizing the protein level of each sample to that of β-actin or albumin.

Measurement of Heparin Binding Affinity of EC-SOD Produced by TRE-*Sod3*-GFP

Because of the added HA-epitope at the C-terminus, we assessed the heparin binding affinity of EC-SOD produced by CMV-*Sod3*-GFP using a published method (Petersen *et al*., 2005). Briefly, heparin affinities were analyzed by affinity chromatography using a 1 ml heparin-Sepharose column (HiTrap Heparin HP; Amersham Biosciences, Piscataway, NJ) connected to an infusion pump (Harvard compact infusion pump model 975) system. Lung homogenate (17 mg) was obtained from WT mouse and was used as a control. A Neuro2A cell clone stably transfected with CMV-*Sod*3-GFP was used to prepare cell lysate for the assay. Fourteen milligram of cell lysate was used. Each sample was diluted five-fold in buffer A (20 mM Tris/HCl containing 5 mM EDTA, pH 7.4) and applied to the column using a 0.6 ml/min flow rate. The column was then washed in 20 ml of buffer A to remove all unbound proteins. Bound proteins were subsequently eluted using a 0.6 ml/min flow rate with a step gradient of NaCl with 50 mM increment from 50 to 600 mM, as well as 1 and 2 M in buffer A. A total of 14 fractions, one from each NaCl concentration, were collected as 1 ml fractions and precipitated with 30% trichloroacetic acid followed by rehydration with 10 μl distilled water. The presence of EC-SOD in each fraction was analyzed by western blot using anti-EC-SOD antibody.

Measurement of SOD Activity

SOD activity was determined based on the nitroblue tetrazolium (NBT) method (Spitz and Oberley, 1989) with some modifications.

Plasma samples—Plasma collected from TRE-*Sod3*-GFP/LAP-tTA double Tg mice (N = 6) and control mice (including WT and two types of single Tg mice, N = 7) were used for SOD activity assay. One-month-old TRE-*Sod3*-GFP/LAP-tTA double Tg mice and control mice were anesthetized (i.p.) with a mixture of ketamine hydrochloride (120 mg/kg) and xylazine (5 mg/kg). Blood was collected through cardiac puncture into a plasma separator tube with lithium heparin (BD Microtainer). Plasma from each sample was obtained by

centrifugation at 10,000 g at room temperature (RT) for 2 min, and stored at −80°C. Because of the presence of high level of xanthine oxidase in the plasma and the low level of circulating SOD activity in nontransgenic mice, we used the value of percent inhibition (% IHB) of NBT reduction to present SOD activity in plasma. Sixty-four microliters of plasma from each mouse was used for a single measurement, triplicate assays were carried out for each sample. Data were presented as the average of % IHB ± SEM (standard error of the mean). The total protein concentration in the plasma was 57.5 ± 3.7 mg/ml and 54.8 ± 3.5 mg/ml for controls and Tg/Tg, respectively; the plasma xanthine oxidase level was 13.2 ± 1.2 mU/ml and 11.8 ± 1.7 mU/ml for controls and Tg/Tg, respectively. There was no significant difference in total plasma protein concentrations or plasma xanthine oxidase levels between the two groups.

Cortex samples—Cortices collected from six TRE-*Sod3*-GFP/CamKII-tTA double Tg and control mice (including WT and two types of single Tg mice) were used to generate samples for the assay. Because EC-SOD is present at very low levels in the brain, cortices from two mice were pooled to make up each sample and the protein in cortex homogenates was partially purified and concentrated based on a published method (Marklund, 1984b, 1990). The process resulted in three independent samples for each Tg/Tg and control group. Briefly, about 0.3 g cortex from each sample was homogenized in 2 ml of ice-cold binding buffer (Tris-HCl 20 mM, NaCl 0.5 M, pH 7.4) followed by sonication (3 × 5 s each, with 5 s pause in between). After the tissue extract was centrifuged at 10,000 g for 5 min at 4°C, the protein concentration of supernatant was determined by BCA method and 1.8 ml of supernatant was applied to a Con A column (Con A-Sepharose, 0.8 ml bed volume, GE Healthcare, Piscataway, NJ). Affinity chromatography was carried out at RT. Glycoprotein fractions containing EC-SOD was eluted by 3 ml elution buffer (Tris-HCl 20 mM, NaCl 0.5 M, 0.5 M methyl α-d-mannopyranoside, pH 6.5) and the column was then washed with the binding buffer. Elution was continuously collected at three drops (~120 μl) per fraction and a total 36 fractions were obtained for each sample. BCA-based protein assay was carried out for all eluted fractions. All samples showed similar amounts of protein in eluted fractions. The protein-containing fractions (fractions 4–28) were pooled and concentrated through Microcon YM-100 centrifugal filter devices (Millipore, Billerica, MA). The presence of EC-SOD in the pooled fractions was confirmed by western blot analysis. Concentrated eluate (~10-fold concentrated) was used for SOD activity assay. As purified EC-SOD was not commercially available, we used CuZnSOD purified from bovine erythrocytes (Sigma) for the generation of a standard curve and defined 1 unit as the amount of SOD required to reach 50% inhibition in the NBT assay system. All assay results were then compared with the standard curve to calculate specific SOD activities. Under the conditions used, 33–50 ng of purified SOD protein was equivalent to 1 unit of SOD activity. Total SOD activity for each sample was calculated based on the total volume of concentrated eluate and normalized to the total protein input into the column.

Immunofluorescence Staining

Immunofluorescence studies were performed to determine the location of EC-SOD expressed in the hippocampal formation of TRE-*Sod3*-GFP/CamKII-tTA double Tg mice. One-month-old mice were sacrificed by cardiac puncture for blood collection, followed by cervical dislocation. The brain was immediately removed and immersed in TBS tissue freezing medium (Triangle Biomedical Sciences, Durham, NC) in a plastic Cryomold. The Cryomold was then floated at RT in isopropanol and cooled down using liquid nitrogen until the sample was completely frozen. The brains were then stored in −80°C until sectioning. Six micrometer cryosections (Leica CM 3050 S) were placed on Superfrost plus slides, fixed in ice-cold methanol for 15 min at −20°C, followed by blocking with 2% BSA in PBS for 30 min at RT. Sections were incubated with primary antibody for 2 h at RT and then detected

with Alexa Fluor-labeled secondary antibodies (Invitrogen). For a double labeling purpose, two primary antibodies were mixed before being applied to the sections, and the same was done for the secondary antibodies. Counterstaining with DAPI (2.5 μg/ml, Invitrogen) was used to visualize nuclei. Antibodies used include anti-EC-SOD (2.5 μg/ml), NeuN (5 μg/ml, MAB377, Chemicon, Temecula, CA), Alexa Fluor 555 goat anti-rabbit IgG (1:200 in PBS, A21428, Invitrogen), and Alexa Fluor 488 goat anti-mouse IgG (1:200 in PBS, A11001, Invitrogen). Images were recorded with an Olympus IX71 inverted fluorescence microscope and merged pictures for double-label staining were created with MetaMorph program (Molecular Devices, Sunnyvale, CA). Brain sections from EC-SOD KO (*Sod3*−/−) mice were used as a background control for EC-SOD antibody.

Dox Administration

To determine Dox-mediated regulation of TRE-*Sod3*-GFP expression in the Tet-Off (TRE-*Sod3*-GFP/LAP-tTA and TRE-*Sod3*-GFP/CamKII-tTA) and Tet-On (TRE-*Sod3*-GFP/CamKII-rtTA) system, Tg/Tg mice were fed Dox-supplemented mouse chow (1,000 ppm, Research Diets Inc., New Brunswick, NJ) starting from 1-month of age. For TRE-*Sod3*-GFP/LAP-tTA mice, only a small quantity of blood was needed for western blot analysis; therefore, a longitudinal study was carried out by collecting blood samples (tail blood, ~10 μl each time) before and at scheduled intervals after the initiation of Dox treatment from the same set of mice. For TRE-*Sod3*-GFP/CamKII-tTA and TRE-*Sod3*-GFP/CamKII-rtTA mice, separate sets of mice were sacrificed before and at scheduled intervals after the initiation of Dox treatment. Recovery of TRE-*Sod3*-GFP expression from the Tet-Off system was carried out by feeding Tg/Tg mice with Dox-supplemented mouse chow to achieve complete suppression, followed by the removal of Dox from the diet. TRE-*Sod3*-GFP expression was then monitored at scheduled intervals after the removal of Dox.

Statistical Analysis

For each endpoint, values for all animals of a given treatment group were averaged and the SEM calculated. The statistical analysis program GraphPad Prism 4 (GraphPad Software, Inc., San Diego, CA) was used for Student's *t* test to compare results from western blot analysis and SOD activity assays.

Acknowledgments

Contract grant sponsor: National Institutes of Health, Contract grant number: AG24400 and NS46051; Contract grant sponsors: Palo Alto Institute for Research and Education (PAIRE) and VA Palo Alto Health Care System

We thank Xinli Wang for excellent animal care and Yanru Chen-Tsai and the Stanford Transgenic Facility for the generation of transgenic mice.

LITERATURE CITED

Bowler RP, Crapo JD. Oxidative stress in airways: is there a role for extracellular superoxide dismutase? Am J Respir Crit Care Med 2002;166:S38–S43. [PubMed: 12471087]

Bowler RP, Nicks M, Olsen DA, Thogersen IB, Valnickova Z, Hojrup P, Franzusoff A, Enghild JJ, Crapo JD. Furin proteolytically processes the heparin-binding region of extracellular superoxide dismutase. J Biol Chem 2002;277:16505–16511. [PubMed: 11861638]

Fattman CL, Schaefer LM, Oury TD. Extracellular superoxide dismutase in biology and medicine. Free Radic Biol Med 2003;35:236–256. [PubMed: 12885586]

Fattman CL, Tan RJ, Tobolewski JM, Oury TD. Increased sensitivity to asbestos-induced lung injury in mice lacking extracellular superoxide dismutase. Free Radic Biol Med 2006;40:601–607. [PubMed: 16458190]

Folz RJ, Abushamaa AM, Suliman HB. Extracellular superoxide dismutase in the airways of transgenic mice reduces inflammation and attenuates lung toxicity following hyperoxia. J Clin Invest 1999;103:1055–1066. [PubMed: 10194479]

Fukai T, Folz RJ, Landmesser U, Harrison DG. Extracellular superoxide dismutase and cardiovascular disease. Cardiovasc Res 2002;55:239–249. [PubMed: 12123763]

Ghio AJ, Suliman HB, Carter JD, Abushamaa AM, Folz RJ. Overexpression of extracellular superoxide dismutase decreases lung injury after exposure to oil fly ash. Am J Physiol Lung Cell Mol Physiol 2002;283:L211–L218. [PubMed: 12060579]

Grill MA, Bales MA, Fought AN, Rosburg KC, Munger SJ, Antin PB. Tetracycline-inducible system for regulation of skeletal muscle-specific gene expression in transgenic mice. Transgenic Res 2003;12:33–43. [PubMed: 12650523]

Hu D, Serrano F, Oury TD, Klann E. Aging-dependent alterations in synaptic plasticity and memory in mice that overexpress extracellular superoxide dismutase. J Neurosci 2006;26:3933–3941. [PubMed: 16611809]

Juul K, Tybjaerg-Hansen A, Marklund S, Heegaard NH, Steffensen R, Sillesen H, Jensen G, Nordestgaard BG. Genetically reduced antioxidative protection and increased ischemic heart disease risk: The Copenhagen City Heart Study. Circulation 2004;109:59–65. [PubMed: 14662715]

Juul K, Tybjaerg-Hansen A, Marklund S, Lange P, Nordestgaard BG. Genetically increased antioxidative protection and decreased chronic obstructive pulmonary disease. Am J Respir Crit Care Med 2006;173:858–864. [PubMed: 16399992]

Kang SK, Rabbani ZN, Folz RJ, Golson ML, Huang H, Yu D, Samulski TS, Dewhirst MW, Anscher MS, Vujaskovic Z. Overexpression of extracellular superoxide dismutase protects mice from radiation-induced lung injury. Int J Radiat Oncol Biol Phys 2003;57:1056–1066. [PubMed: 14575837]

Katsantoni EZ, Anghelescu NE, Rottier R, Moerland M, Antoniou M, de Crom R, Grosveld F, Strouboulis J. Ubiquitous expression of the rtTA2S-M2 inducible system in transgenic mice driven by the human hnRNPA2B1/CBX3 CpG island. BMC Dev Biol 2007;7:108. [PubMed: 17900353]

Kistner A, Gossen M, Zimmermann F, Jerecic J, Ullmer C, Lubbert H, Bujard H. Doxycycline-mediated quantitative and tissue-specific control of gene expression in transgenic mice. Proc Natl Acad Sci USA 1996;93:10933–10938. [PubMed: 8855286]

Li L, Miano JM, Mercer B, Olson EN. Expression of the SM22α promoter in transgenic mice provides evidence for distinct transcriptional regulatory programs in vascular and visceral smooth muscle cells. J Cell Biol 1996;132:849–859. [PubMed: 8603917]

Mansuy IM, Winder DG, Moallem TM, Osman M, Mayford M, Hawkins RD, Kandel ER. Inducible and reversible gene expression with the rtTA system for the study of memory. Neuron 1998;21:257–265. [PubMed: 9728905]

Marklund SL. Extracellular superoxide dismutase and other superoxide dismutase isoenzymes in tissues from nine mammalian species. Biochem J 1984a;222:649–655. [PubMed: 6487268]

Marklund SL. Extracellular superoxide dismutase in human tissues and human cell lines. J Clin Invest 1984b;74:1398–1403. [PubMed: 6541229]

Marklund SL. Analysis of extracellular superoxide dismutase in tissue homogenates and extracellular fluids. Methods Enzymol 1990;186:260–265. [PubMed: 2233298]

Mayford M, Bach ME, Huang YY, Wang L, Hawkins RD, Kandel ER. Control of memory formation through regulated expression of a CaMKII transgene. Science 1996;274:1678–1683. [PubMed: 8939850]

Oury TD, Day BJ, Crapo JD. Extracellular superoxide dismutase in vessels and airways of humans and baboons. Free Radic Biol Med 1996;20:957–965. [PubMed: 8743981]

Oury TD, Ho YS, Piantadosi CA, Crapo JD. Extracellular superoxide dismutase, nitric oxide, and central nervous system O2 toxicity. Proc Natl Acad Sci USA 1992;89:9715–9719. [PubMed: 1329105]

Oury TD, Piantadosi CA, Crapo JD. Cold-induced brain edema in mice. Involvement of extracellular superoxide dismutase and nitric oxide. J Biol Chem 1993;268:15394–15398. [PubMed: 7687996]

Passman RS, Fishman GI. Regulated expression of foreign genes in vivo after germline transfer. J Clin Invest 1994;94:2421–2425. [PubMed: 7989599]

Petersen SV, Olsen DA, Kenney JM, Oury TD, Valnickova Z, Thogersen IB, Crapo JD, Enghild JJ. The high concentration of Arg213– >Gly extracellular superoxide dismutase (EC-SOD) in plasma is caused by a reduction of both heparin and collagen affinities. Biochem J 2005;385:427–432. [PubMed: 15362977]

Rabbani ZN, Anscher MS, Folz RJ, Archer E, Huang H, Chen L, Golson ML, Samulski TS, Dewhirst MW, Vujaskovic Z. Overexpression of extracellular superoxide dismutase reduces acute radiation induced lung toxicity. BMC Cancer 2005;5:59. [PubMed: 15949035]

Rola R, Zou Y, Huang TT, Fishman K, Baure J, Rosi S, Milliken H, Limoli CL, Fike JR. Lack of extracellular superoxide dismutase (EC-SOD) in the microenvironment impacts radiation-induced changes in neurogenesis. Free Radic Biol Med 2007;42:1133–1145. Discussion 1131–1132. [PubMed: 17382195]

Sandstrom J, Nilsson P, Karlsson K, Marklund SL. 10-fold increase in human plasma extracellular superoxide dismutase content caused by a mutation in heparin-binding domain. J Biol Chem 1994;269:19163–19166. [PubMed: 8034674]

Sarao R, Dumont DJ. Conditional transgene expression in endothelial cells. Transgenic Res 1998;7:421–427. [PubMed: 10341450]

Sheng H, Bart RD, Oury TD, Pearlstein RD, Crapo JD, Warner DS. Mice overexpressing extracellular superoxide dismutase have increased resistance to focal cerebral ischemia. Neuroscience 1999;88:185–191. [PubMed: 10051199]

Sheng H, Kudo M, Mackensen GB, Pearlstein RD, Crapo JD, Warner DS. Mice overexpressing extracellular superoxide dismutase have increased resistance to global cerebral ischemia. Exp Neurol 2000;163:392–398. [PubMed: 10833313]

Spitz DR, Oberley LW. An assay for superoxide dismutase activity in mammalian tissue homogenates. Anal Biochem 1989;179:8–18. [PubMed: 2547324]

Suliman HB, Ryan LK, Bishop L, Folz RJ. Prevention of influenza-induced lung injury in mice overexpressing extracellular superoxide dismutase. Am J Physiol Lung Cell Mol Physiol 2001;280:L69–L78. [PubMed: 11133496]

Thiels E, Urban NN, Gonzalez-Burgos GR, Kanterewicz BI, Barrionuevo G, Chu CT, Oury TD, Klann E. Impairment of long-term potentiation and associative memory in mice that overexpress extracellular superoxide dismutase. J Neurosci 2000;20:7631–7639. [PubMed: 11027223]

Thomas MK, Devon ON, Lee JH, Peter A, Schlosser DA, Tenser MS, Habener JF. Development of diabetes mellitus in aging transgenic mice following suppression of pancreatic homeoprotein IDX-1. J Clin Invest 2001;108:319–329. [PubMed: 11457885]

Tichelaar JW, Lu W, Whitsett JA. Conditional expression of fibroblast growth factor-7 in the developing and mature lung. J Biol Chem 2000;275:11858–11864. [PubMed: 10766812]

van der Bijl P, Pitigoi-Aron G. Tetracyclines and calcified tissues. Ann Dent 1995;54:69–72. [PubMed: 8572553]

Wang J, Lin W, Popko B, Campbell IL. Inducible production of interferon-γ in the developing brain causes cerebellar dysplasia with activation of the Sonic hedgehog pathway. Mol Cell Neurosci 2004;27:489–496. [PubMed: 15555926]

West J, Fagan K, Steudel W, Fouty B, Lane K, Harral J, Hoedt-Miller M, Tada Y, Ozimek J, Tuder R, Rodman DM. Pulmonary hypertension in transgenic mice expressing a dominant-negative BMPRII gene in smooth muscle. Circ Res 2004;94:1109–1114. [PubMed: 15031260]

Zheng T, Zhu Z, Wang Z, Homer RJ, Ma B, Riese RJ Jr, Chapman HA Jr, Shapiro SD, Elias JA. Inducible targeting of IL-13 to the adult lung causes matrix metalloproteinase- and cathepsin-dependent emphysema. J Clin Invest 2000;106:1081–1093. [PubMed: 11067861]

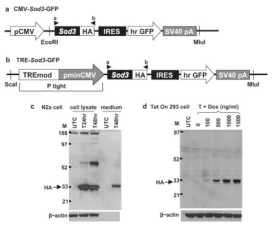

FIG. 1.

Sod3 expression constructs and in vitro expression. (**a**) CMV-*Sod3*-GFP and (**b**) TRE-*Sod3*-GFP constructs. Promoters and coding sequences are shown in shaded boxes and the backbone of cloning vectors is shown in black thick lines. Locations of restriction sites used for cloning are indicated. Locations of primers used for TRE-*Sod3*-GFP genotyping are marked by arrowheads a and b. (**c**) Expression of CMV-*Sod3*-GFP in transiently transfected Neuro2A cells. Cell lysates collected at 24 (T24hr) and 48 (T48hr) h, as well as culture medium collected at 48 h after transfection were used for western blot analysis. (**d**) Expression of TRE-*Sod3*-GFP in transiently transfected Tet-On 293 cells. Various amounts of Dox were added at the time of transfection to induce the expression of EC-SOD. Cell lysates were collected at 48 h after transfection and used for western blot analysis. Anti-HA antibody was used for the detection of HA-tagged EC-SOD. T, transfected; UTC, untransfected control; N2a, Neuro2A; M, molecular weight marker.

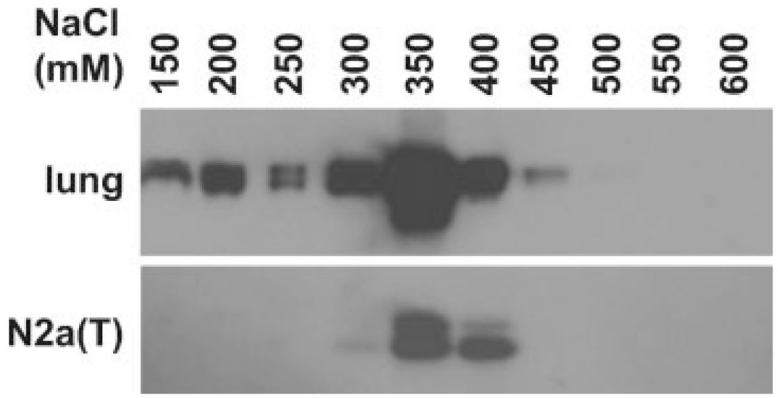

FIG. 2.

Heparin binding affinity of HA-tagged EC-SOD. Eluted fractions from lung homogenate and from Neuro2A cell stably transfected with CMV-*Sod3*-GFP were collected through a heparin-sepharose column and analyzed by western blot using anti-EC-SOD antibody. N2a, Neuro2A cells.

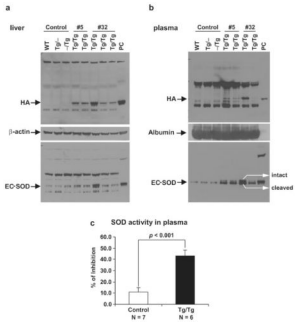

FIG. 3.

Increased EC-SOD expression and SOD activity in TRE-*Sod3*-GFP/LAP-tTA double transgenic mice. Increased expression of transgenic EC-SOD was detected in liver homogenates (**a**) and plasma (**b**) from Tg/Tg but not from control mice (WT, Tg/−, and −/Tg). Both transgenic lines (#5 and #32) showed similar expression level. β-actin and albumin were used as internal controls for liver and plasma protein loading, respectively. Anti-HA and a custom-made anti-EC-SOD antibody were used for western blot analyses. The larger, tissue-bound (intact) form of EC-SOD and the smaller, cleaved from of EC-SOD can be distinguished in this western blot. As typical of the circulating EC-SOD, the cleaved EC-SOD is the dominant form. WT, nontransgenic; Tg/−, TRE-*Sod3*-GFP single transgenic; −/Tg, LAP-tTA single transgenic; Tg/Tg, TRE-*Sod3*-GFP/LAP-tTA double transgenic; PC, positive control using cell lysate from Neuro2A cells stably transfected with CMV-*Sod3*-GFP. (**c**) Total SOD activity was measured in plasma from TRE-*Sod3*-GFP/LAP-tTA mice (line #5). A 3.9-fold ($P < 0.001$) increase in SOD activity was detected in the plasma of Tg/Tg mice compared with control mice (WT, Tg/−, and −/Tg).

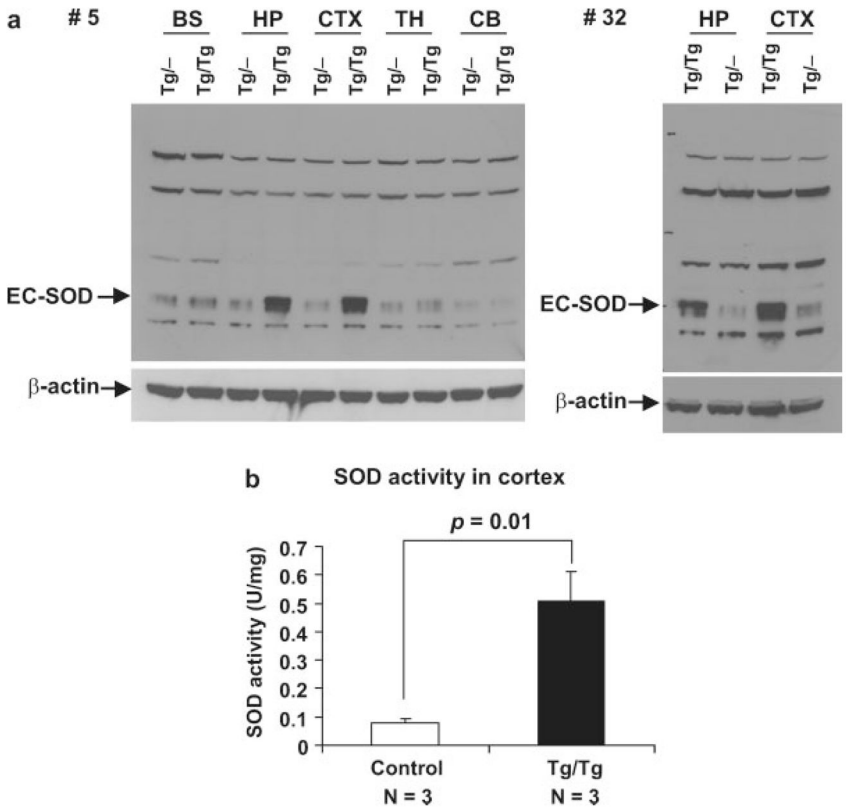

FIG. 4.

Increased EC-SOD expression and SOD activity in TRE-*Sod3*-GFP/CamKII-tTA double Tg mice. (**a**) Increased expression of transgenic EC-SOD was detected in dissected brain regions from TRE-*Sod3*-GFP/CamKII-tTA double Tg mice. The increased transgene expression was only detected in hippocampus and cortex of Tg/Tg and not in that of control mice (Tg/−). Representative results are shown. EC-SOD-specific signals were indicated by an arrow; the additional bands were nonspecific signals. (**b**) EC-SOD activity was measured in cortex homogenates from TRE-*Sod3*-GFP/CamKII-tTA mice line #5. A 6.4-fold (P = 0.01) increase in SOD activity was detected in the cortex of Tg/Tg mice compared with control mice (WT, Tg/−, and −/Tg). Tg/−, TRE-*Sod3*-GFP single transgenic; −/Tg, CamKII-tTA single transgenic; Tg/Tg, TRE-*Sod3*-GFP/CamKII-tTA double transgenic; BS, brain stem; HP, hippocampus; CTX, cortex; TH, thalamus; CB, cerebellum.

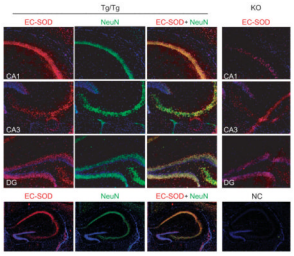

FIG. 5.

Location of EC-SOD in hippocampus from TRE-*Sod3*-GFP/CamKII-tTA double Tg mice. EC-SOD is colocalized with NeuN in hippocampus in CA1, CA3, and DG. Left panels show the immunofluorescence staining for EC-SOD (red), NeuN (green), and the merged images in hippocampus from Tg/Tg, with the comparison to that from EC-SOD KO (top three photos on the right). A negative control (NC) stained with secondary antibody only is presented at the bottom right hand corner. Slides were counterstained with DAPI (blue). Tg/Tg, TRE-*Sod3*-GFP/CamKII-tTA double transgenic; KO, EC-SOD knockout mouse; CA1 and CA3, Cornu Ammonis area 1 and 3; DG, dentate gyrus; NeuN, neuronal nuclei.

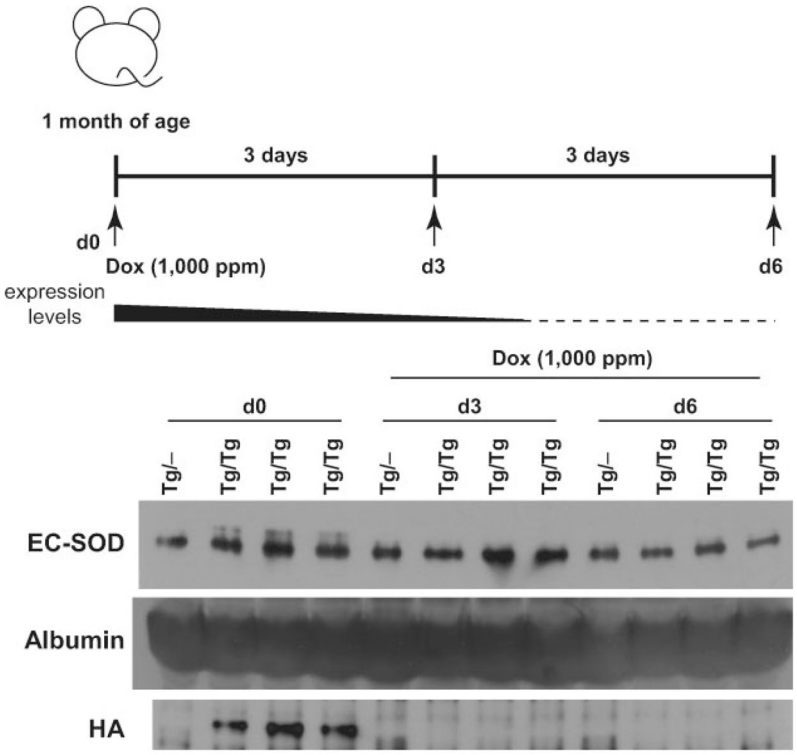

FIG. 6.

Suppression of EC-SOD expression by Dox-supplemented mouse chow in TRE-*Sod3*-GFP/LAP-tTA mice. Upper panel, the time line for longitudinal blood collection before (Day 0) and after the initiation of Dox treatment. Middle panel, a graphical presentation of EC-SOD levels in response to Dox treatment. The solid area corresponds to the proportional level of EC-SOD from the transgenes and the dash line represents the endogenous EC-SOD. Lower panel, western blot analysis of plasma EC-SOD levels in control (Tg/−) and Tg/Tg mice before and after Dox treatment. Albumin was used as an internal control for plasma protein loading. Tg/−, TRE-*Sod3*-GFP single transgenic; Tg/Tg, TRE-*Sod3*-GFP/LAP-tTA double transgenic. Data from three independent Tg/Tg mice are shown.

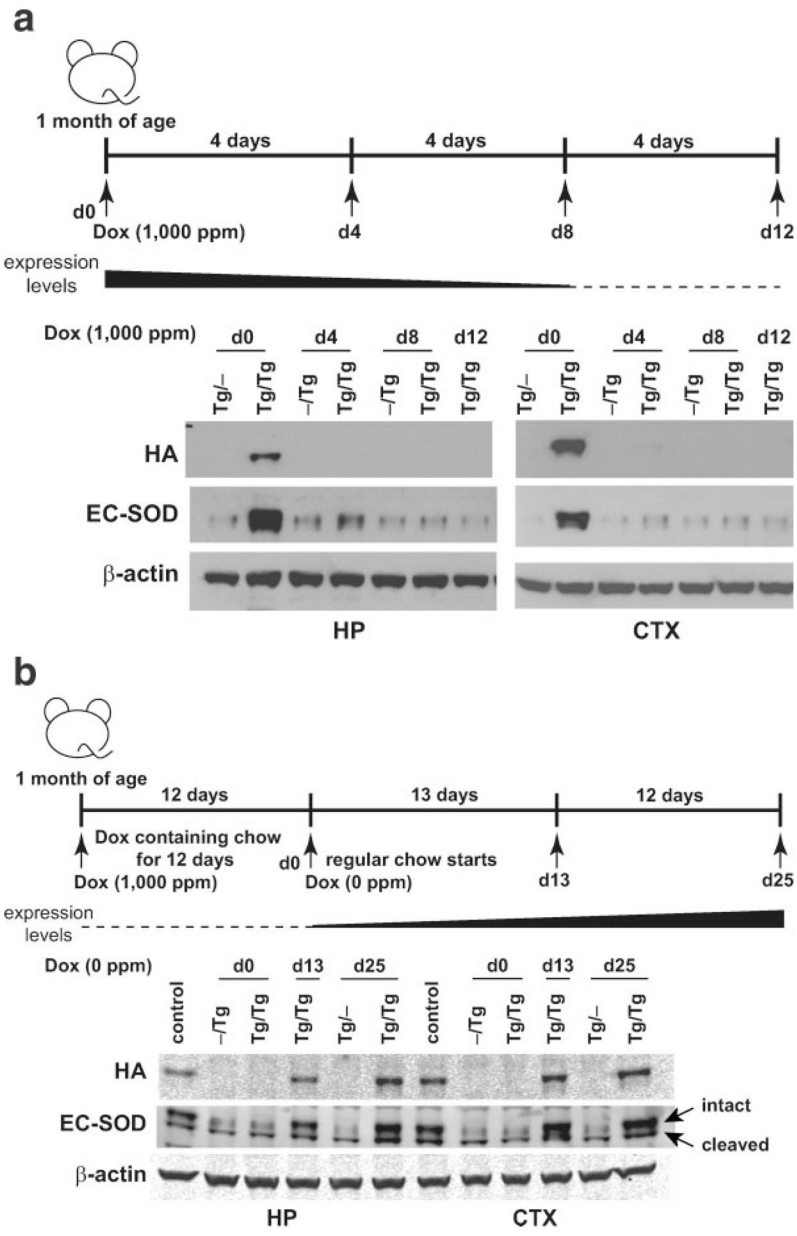

FIG. 7.

Reversible suppression of EC-SOD by Dox in TRE-*Sod3*-GFP/CamKII-tTA mice. (**a**) Suppressed expression of EC-SOD in Tg/Tg mice. Upper panel, the time line for sample collection before (Day 0) and after the initiation of Dox treatment. Middle panel, a graphical presentation of EC-SOD level in response to Dox treatment. Lower panel, western blot analysis of EC-SOD expression in hippocampus and cortex. (**b**) Recover of TRE-*Sod3*-GFP expression after removal of Dox-supplementation. Upper panel, the time line for sample collection before and after the initiation and termination of Dox treatment. Middle panel, a graphical presentation of EC-SOD level in response to Dox treatment. Lower panel, western blot analysis of EC-SOD expression in hippocampus and cortex. The intact and cleaved EC-SOD are well separated in this western blot and shows the typical pattern in brains with intact EC-SOD as the dominant form. Control: Tg/Tg never treated with Dox; Tg/−, TRE-

Sod3-GFP single transgenic; −/Tg, CamKII-tTA single transgenic; Tg/Tg, TRE-*Sod3*-GFP/LAP-tTA double transgenic; HP, hippocampus; CTX, cortex.